Prediction of Fatigue Crack Propagation Life in Notched Members under Variable Amplitude Loading

Z. Khan, A. Rauf, and M. Younas

One of the interesting phenomenon in the study of fatigue crack propagation under variable amplitude load cycling is the crack growth retardation that normally occurs due to the application of a periodic overload. Fatigue crack growth rate under simple variable amplitude loading sequence incorporating period overloads is studied using single edge notched specimens of AISI 304 stainless steel. Load interaction effects due to single and multiple overload have been addressed. Substantial retardation of fatigue crack growth rate is observed due to the introduction of periodic tensile overloads. Estimates of fatigue life have been obtained employing Wheeler model (using Paris and modified Paris equations) and Elber's model. Analytical predictions are compared with experimental results. Results of these analytical fatigue life predictions show good agreement with the experimental fatigue life data. Fatigue crack propagation rates also have been evaluated from the fractographic study of fatigue striations seen on the fracture surface. Good agreement was found between the experimentally observed crack growth rates and the fatigue crack growth rates determined by the fractographic studies.

Keywords
crack propagation, life prediction, notched member, variable amplitude

1. Introduction

DURING THE PAST twenty-five years, extensive effort has been devoted to developing methodologies that permit the prediction of fatigue lives by different analytical models. Because crack-like defects or discontinuities such as voids, inclusions, geometric stress raisers, and weld defects are inherently present in a given structure, the crack initiation portion of the total fatigue life becomes less significant than the crack propagation portion. In such situations, the prediction of fatigue crack propagation becomes a primary concern. A good technique to predict fatigue crack propagation lives thus becomes an important tool from a design as well as a service point of view of component and structures subjected to cyclic loading. Crack growth predictions are most often used to evaluate the damage tolerance to extend the service life of structures, to establish inspection controls, and to analyze failure.

It is well known that most engineering structures and components are subjected to variable amplitude load cycling. Prediction models that attempt to estimate fatigue life have to

Z. Khan, A. Rauf, and **M. Younas,** Mechanical Engineering Department, King Fahd University of Petroleum and Minerals, Dhahran, Saudi Arabia.

Nomenclature

a	crack length	p	Wheeler's shaping exponent
a_f	final crack length	P	applied load
a_i	initial crack length	ΔP	range of applied load
a_o	crack length before the overload	P_{max}	maximum load applied in the cycle
a_p	sum of crack length before the OL and the OL plastic zone size	P_{mean}	mean load of cycle
		P_{min}	minimum load applied in the cycle
C	Paris constant	r_y	plastic zone size
C_p	Wheeler's retardation coefficient	r_{OL}	overload plastic zone size
da/dN	fatigue crack growth rate	R	stress ratio
$f(g)$	the geometric factor	t	thickness of the specimen
K_c	fracture toughness	U	effective stress parameter
K_{max}	maximum stress intensity	w	width of the specimen
K_{OL}	stress intensity factor at the overload	ρ	radius of the notch
ΔK	stress intensity factor range	σ	nominal stress at crack tip
ΔK_{eff}	effective stress intensity factor	σ_{alt}	mean stress at the crack tip
m	Paris coefficient (slope of crack growth curve)	σ_{max}	maximum stress at crack tip
		σ_{mean}	mean stress at crack tip
n	number of cycles in the base constant amplitude cycle	σ_{min}	minimum stress at crack tip
		σ_{OP}	crack opening stress
N	total number of life cycles	σ_{YS}	tensile yield strength of the material
N_p	number of crack propagation life cycle		

satisfy criteria that determine their ability to predict the fatigue life under various variable amplitude load histories and to consider the material behavior with the mechanistic aspect of fatigue. Presently available fatigue life prediction concepts require not only the baseline constant amplitude loading (CAL) data, but also variable amplitude loading (VAL) data to arrive at reliable fatigue life predictions with reasonable accuracies.

Of particular interest is the study of crack growth is a load history where constant amplitude load cycling is followed by an overload (OL) load excursion. Under CAL, fatigue crack propagation is dependent only on the present crack size and the applied load. However, under VAL conditions, fatigue crack propagation is also dependent on the preceding loading history. This dependence is termed *load interaction effect.* It is defined as deviations of the actual crack growth rate per cycle under VAL history from crack growth rate as predicted on the basis of constant amplitude crack growth data.

The consequence of this effect may be observed as retardation, acceleration, or arresting of the growing crack. Hence, load interaction significantly affects the fatigue crack growth (FCG) rate and consequently the fatigue life. Even the application of a single tensile OL within a CAL block can produce a marked retardation in the FCG rate. Crack retardation remains in effect for a period of loading after the OL cycle(s) is (are) applied. The number of cycles in this period has been shown to correspond to the plastic zone size developed due to the OL. It has been shown that the number of cycles in the CAL block, the OL or the underload (UL) stress magnitude, and the number of the overload cycles have a significant effect on the fatigue crack propagation life (Ref 1). If the OL magnitude is large enough, the growth temporarily stops. This phenomenon is called *crack arrest.* The OL produces a new, larger plastic zone at the crack tip responsible for the arresting of the growing crack.

Some controversial issues are reported in the findings of single OL applied in a VAL loading history (Ref 2). One group of researchers reports that retardation increases with increase in the baseline loading range ΔK for a given overload ratio (Ref 3-5), whereas another group observed that retardation decreases with increase in the baseline loading range for similar conditions (Ref 6-8).

In this study, the effect of the tensile OL cycles on the FCG rates has been investigated. Two analytical models, the Wheeler's model and Elber's model, applicable to VAL cycling have been employed to predict the fatigue crack propagation (FCP) life. Paris and modified Paris equations are used in the Wheeler's model.

2. Analytical Formulation

Fatigue crack propagation under VAL is significantly influenced by the preceding load cycles (the interaction effect). Therefore, the CAL models cannot provide satisfactory estimates of the fatigue lives of components in actual service conditions. Linear elastic fracture mechanics principles have been used successfully to relate stress magnitude and distribution near the crack tip to the remote stress applied to the cracked component, the crack size and shape, and the material properties of the cracked component.

Fatigue lives of a critically loaded part are conservatively predicted by integration of a relationship describing the crack growth rate as a function of mechanical crack driving force from initial to final crack size. For nominally linear elastic conditions, where driving force can be defined in terms of the applied ΔK, this relation is given by the Paris equation:

$$\frac{da}{dN} = C(\Delta K)^m \qquad \text{(Eq 1)}$$

where C and m are material constants. Wheeler (Ref 9) suggested that retardation in the crack growth rate following an OL under VAL conditions may be predicted by modifying the CAL growth rate. This means that an already existing FCG rate model developed for CAL studies can be used by incorporating a factor dependent on the interaction effect. Unfortunately, this requires a shaping parameter p, which has to be obtained experimentally for different materials.

The stress intensity factor ΔK using the fracture mechanics concept is given as:

$$\Delta K = f(g)\Delta\sigma\sqrt{\pi a} \qquad \text{(Eq 2)}$$

where $f(g)$ is a geometric correction parameter, $\Delta\sigma$ is the global stress range (MPa), a is the instantaneous crack length. According to Wheeler's model, Eq 1 can be written in terms of constant amplitude growth rate with a retardation parameter C_p as:

$$\frac{da}{dN_i} = (C_p)_i\left(\frac{da}{dN}\right)CA_i \qquad \text{(Eq 3)}$$

where $(da/dN)CA_i$ is a constant amplitude growth rate approximated by the stress intensity factor range ΔK_i, and the retardation parameter $(C_p)_i$ is a function of the ratio of current plastic zone size to the plastic zone size created by the OL, given by:

$$(C_p)_i = \left(\frac{r_{yi}}{a_p - a_i}\right)^p \qquad \text{(Eq 4)}$$

where r_{yi} is the cyclic plastic zone size due to the ith loading cycle, p is an empirically determined shaping parameter, a_i is the crack length at the ith loading cycle, and a_p is the sum of the crack length at which the OL occurred and the OL plastic zone size given by $(a_p - a_i) = a_o - a_i = a_i + r_{OL} - a_i$. Assuming that the crack length just before the OL is relatively close to the crack length at which OL occurred, then, $a_p \approx r_{OL}$ (Ref 10, 11). This corresponds to assuming that $(C_p)_i \approx C_p$, where C_p is the average value.

According to Wheeler's model, retardation decreases proportionally to the penetration of the crack into the OL zone with maximum retardation occurring immediately after the OL. The values of $(C_p)_i$ range from 0.01 to 1.0. Crack retardation is assumed to occur as long as the current plastic zone size is within the plastic zone created by the OL. As soon as the boundary of the current plastic zone touches the boundary of the OL zone,

retardation is assumed to cease, which corresponds to $(C_p)_i = 1.0$, and the retardation is maximum at $(C_p)_i = 0$.

In Eq 3, the constant amplitude crack growth rate can be found using the Paris relation in Eq 1 and the stress intensity factor given by Eq 2. The integration of this crack growth equation with reference to the crack length a yields the theoretical value of fatigue crack propagation life (N_p) as predicted by Wheeler's model using the Paris equation given by:

$$N_p = \int_{a_i}^{a_f} \frac{1}{(C_p)^p\, C(f(g)\Delta\sigma\sqrt{\pi a})^m}\, da \qquad \text{(Eq 5)}$$

where a_i is the initial (precracking) crack length and a_f is the final fracture crack length given by:

$$a_f = \frac{w}{2} - \frac{P_{max}}{2t\sigma_{YS}} \qquad \text{(Eq 6)}$$

where w is the width of the specimen, t is the specimen thickness, and P_{max} is the maximum load applied during the constant amplitude part of the cycle.

Allen (Ref 12) reported that fatigue life for various steels under VAL is influenced by the stress ratio R. The CAL relation given by Paris (Eq 1) was modified by:

$$\frac{da}{dN} = \frac{1+R}{1-R} C(\Delta K)^m \qquad \text{(Eq 7)}$$

where C and m are the Paris constants found by the constant amplitude loading test, R is the stress ratio given by $(\sigma_{min}/\sigma_{max})$, and ΔK is given by Eq 2.

The integration of Eq 6 (with a_f same as in Eq 5) will yield the predicted fatigue crack propagation life using Wheeler's equation:

$$N_p = \int_{a_i}^{af} \frac{(1-R)/(1+R)}{(C_P)^p\, C(\Delta K)^m}\, da \qquad \text{(Eq 8)}$$

Elber's model (Ref 13) presented that the FCG rate model under VAL utilizes the compressive residual stress at the crack tip to predict FCG rate. Stresses are developed due to the elastic body surrounding the OL plastic zone, which causes these zones to go into compression after removal of the OL. The crack is assumed to propagate in the tensile portion of the cycle; in the compressive portion, it is assumed to be closed and not propagating.

The basic crack growth rate equation (Eq 1) can be the same as the one used by Paris with some modifications to accommodate the effective stress concept. Hence, the required effective stress intensity range (ΔK_{eff}) is given by:

$$\Delta K_{eff} = U\Delta K \qquad \text{(Eq 9)}$$

Although U may be taken as a complicated function varying from cycle to cycle and from one loading condition to another, for conventional fatigue programs U can be assumed to be quite simple and a function of R only (Ref 9).

$$U = 0.618 + 0.365R + 0.139R^2 \qquad \text{(Eq 10)}$$

The above effective stress relation is incorporated in order to account for the crack opening behavior using ΔK_{eff} (Eq 9). This relation was obtained from the data by linear regression for $R \geq 0$, which is satisfied by the present loading conditions as well. Many authors have used this and similar relations to give satisfactory results close to the experimental findings (Ref 10, 11).

Using the preceding relations and Eq 1, FCP lives from Elber's model can be calculated as:

$$N_p = \int_{a_i}^{a_f} \frac{1}{C(U\Delta K)^m}\, da \qquad \text{(Eq 11)}$$

The fatigue crack growth rates were also determined from the fracture surface studies using scanning electron microscopy. The crack growth rate is calculated using (Ref 18):

$$\frac{da}{dN} = \frac{1}{\text{Magnification}} \times \frac{\text{Distance on the fractograph}}{\text{Striation count / unit distance on the fractograph}} \qquad \text{(Eq 12)}$$

3. Collection of Data

To obtain the necessary fatigue crack propagation data, 120 × 38 × 1.5 mm thick, single-edge notched specimens of stainless steel type AISI 304L were used. The chemical composition of the alloy is provided in Table 1. The specimen geometry is shown in Fig. 1. A servohydraulic materials test system was used for carrying out all the fatigue tests. The specimens were cyclically loaded in the direction parallel to the rolling direction. All crack growth measurements were made using a long distance traveling microscope. The specimens were precracked under fatigue loading to a length of 0.001 m before the crack growth rate measurements were started. For clarity of observation of the crack, the surfaces of the samples were hand polished using successively finer emery paper to a final 600 grit emery paper polish. The final polish was done in the direction perpendicular to the crack growth direction. The two loading histories used in this investigation were a single tensile OL and multiple tensile OL, which were superimposed on baseline constant amplitude loading cycles. All tests were thus composed of two tasks per block. The constant amplitude part running for n number of sinusoidal cycles at 10 Hz was followed by a single OL part at 0.1 Hz, which was one-half of the sine cycle. These blocks were repeated to generate the VAL loading history at 10 Hz. P_{mean} was 4 kN and amplitude ±3 kN (giving ΔP as 6 kN, P_{max} as 7 kN, and P_{min} as 1 kN). The number of cycles (n) in the constant amplitude (CA) part ranged from 5000, 1000, and 100, with the peak OL at 9 kN for sample numbers 4,

5, and 6, respectively. To observe the effect of the magnitude of OL, the OL was raised to 11 kN and 13 kN for sample numbers 10 and 11, respectively. Besides single overloads, some multiple overloads were also used.

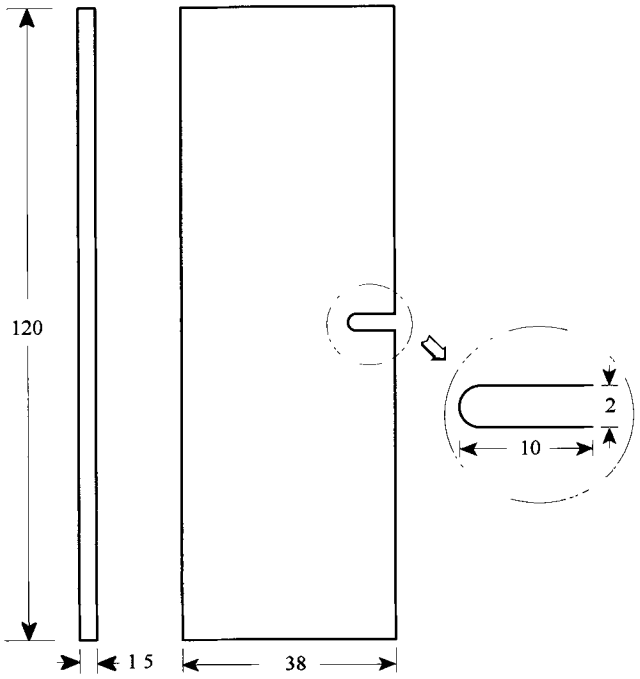

Fig. 1 Geometry of the FCGR specimen

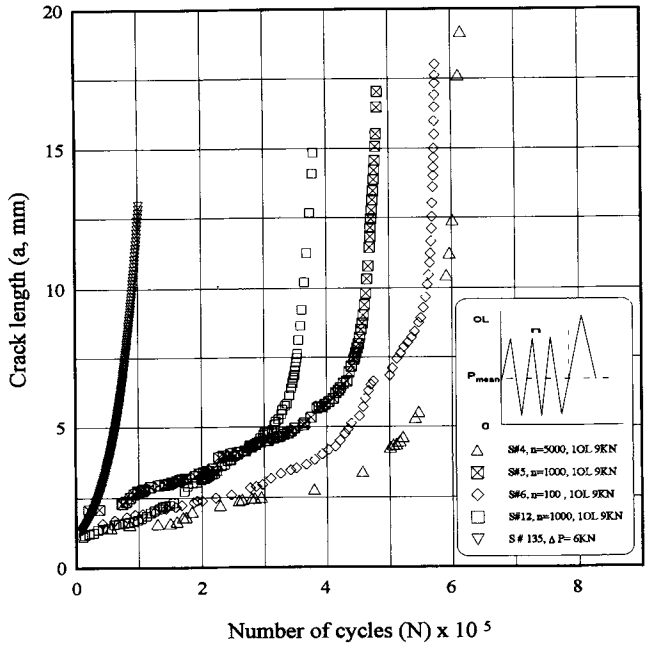

Fig. 2 Effect of the number of constant amplitude cycles on the fatigue crack growth retardation

4. Results and Discussion

With the decrease in the base number of CAL cycles (n) from n = 5000 to n = 1000, the fatigue life is decreased considerably, but further decrease in the number of base CAL cycles to n = 100 shows an increase in the fatigue life compared to n = 1000 cycles. This trend is closer to n = 5000 cycles (Fig. 2). The corresponding FGG rate plots showing the effect of numbers of CAL is shown in Fig. 3.

Under similar conditions, when the magnitude of OL is increased from 9 kN (OL ratio 1.5) to 13 kN (OL ratio 2.17), the fatigue life is decreased as shown in Fig. 4. At 13 kN the a versus N curve becomes almost identical to the CAL curve. This means that the retardation effect due to overload diminishes at OL ratio 2.17. A similar observation was also reported by Crysler et al. (Ref 14). The corresponding da/dN versus ΔK plots showing the effect of number of base cycles on FCG rate is shown in Fig. 5.

When the FCG curve is analyzed, it is observed that the FCG rate increases with the increase in the magnitude of OL. However, the crack growth retardation is still observed at the OL when compared with CAL (Fig. 5). Jones (Ref 15) has also reported that the OL ratio could also be used as an indication of the amount of subsequent retardation.

Number of OL peaks when increased from one to five, each with the same magnitude, still produces retardation in the crack growth rate when compared to the CAL under the same conditions (see Fig. 6) and produces an acceleration in the FCG rate when compared to the single overload. Figure 7 shows the corresponding FCG rate plots.

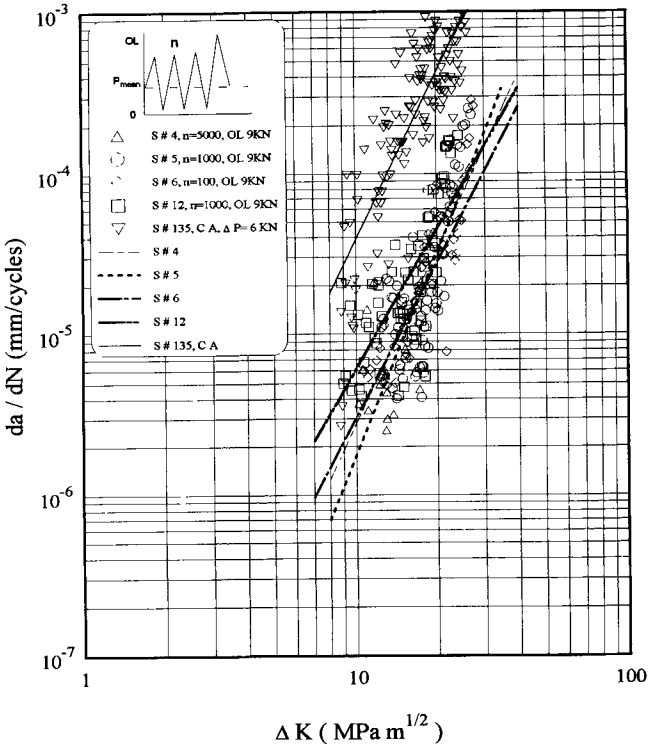

Fig. 3 FCG rate versus ΔK showing the effect of number of base cycles

Residual compressive stresses that are produced by the surrounding elastic material are decreased as the number of overloads increases. This causes the crack to travel a shorter distance in the plastic zone; hence it is not as retarded as under single OL. Crack closure effects are also reduced with multiple OL application as compared to single OL. Fatigue crack growth rate retardation has been observed to occur in all the fatigue tests carried out under this investigation. The magnitude of crack growth retardation ranged from very substantial to modest under different conditions of constant amplitude overload combinations.

Figure 2 presents the results of the fatigue tests in which a single tensile overload of 9 kN was applied after each block of constant amplitude cycling in which the constant amplitude cycles were increased from 100 to 1000 and then to 5000. As shown in Fig. 2, the largest degree of crack growth retardation is observed when the single tensile overload is applied after 5000 cycles. When the number of constant amplitude cycles was reduced to 1000, the magnitude of crack growth retardation decreased, suggesting that the number of constant amplitude cycles preceding the overload cycle has a significant effect on the FCG rates. This reduced retardation effect observed when the overload cycle is introduced quicker (after 1000 CA cycles) rather than after 5000 CA cycles could be attributed to the difference in the conditions in which the FCG takes place after the application of the overload cycle. In both cases, the application of the overload of the same magnitude can be assumed to produce similar plastic zones. The crack after the application of the overload must then grow under constant amplitude cycling through the plastic zone created by the overload. It is known that crack growth acceleration takes place immediately after the overload, which is followed by a significant drop in the growth rates.

This reduced crack growth, which occurs under the constant amplitude cycling preceding the overload, should be favored if a larger number of constant amplitude cycles are applied before the next overload is introduced. A lower number of constant amplitude cycles would offset the period of delayed retardation by bringing the next crack growth acceleration event before the full realization of the crack growth retardation is achieved. This should mean that a further decrease in the number of constant amplitude cycles, which precedes the overload, must be expected to further minimize the retardation effects. Contrary to this expectation, a decrease in the number of constant amplitude cycles from $n = 1000$ to $n = 100$, instead of exhibiting a higher fatigue crack growth rate as compared to the fatigue crack growth rate for $n = 1000$, shows a lower fatigue crack growth rate. This suggests that application of a small number of constant amplitude cycles ($n = 100$) preceding the overload produces a more effective retardation than the retardation produced by a moderately larger number of constant amplitude cycles ($n = 1000$) preceding the overload. This retardation in the crack

Table 1 Chemical composition and mechanical properties of AISI 304L stainless steel

Steel	Chemical composition, wt %						Yield strength, MPa	Tensile strength, MPa	Elongation, %
	Ni	Si	Mn	Cr	S	Cu			
AISI 304L	9.20	0.40	1.70	19.30	0.01	0.20	20	515	30

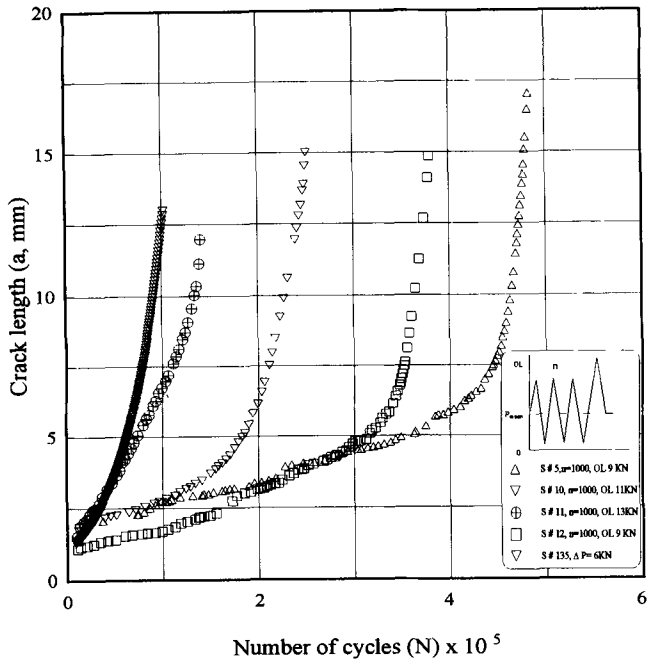

Fig. 4 Effect of overload magnitude on the fatigue crack retardation

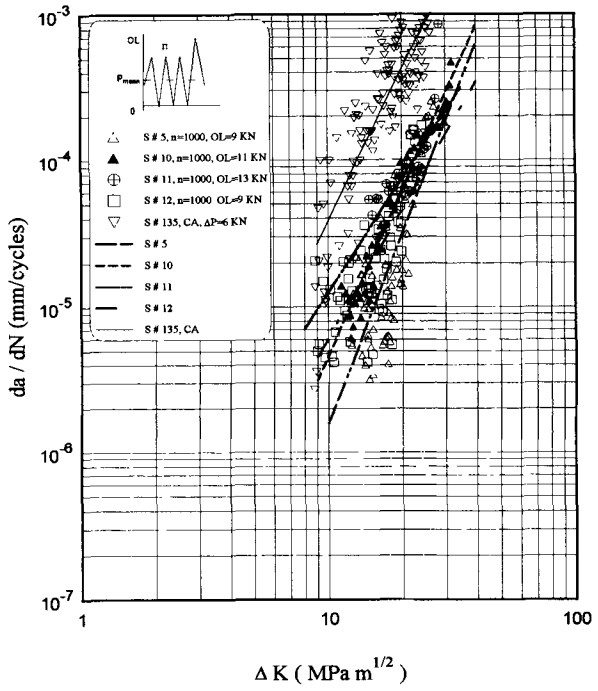

Fig. 5 FCG rate versus ΔK showing overload magnitude effect

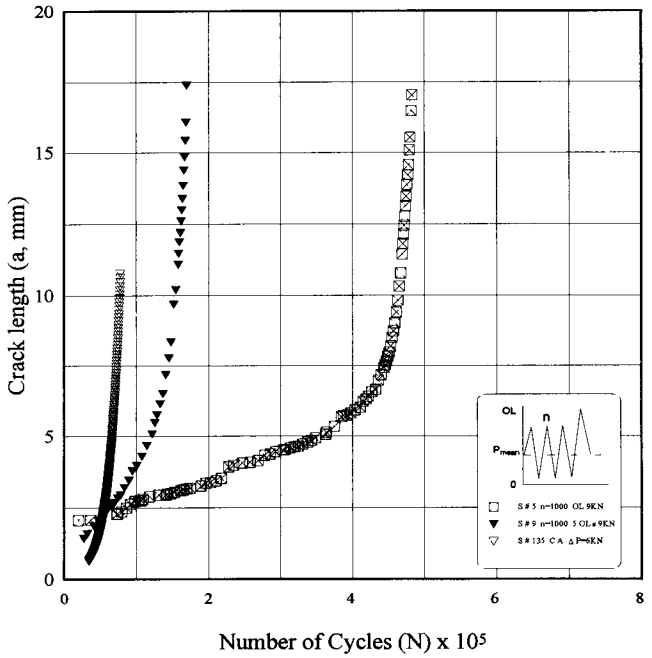

Fig. 6 Effect of the number of overload cycles on the fatigue crack growth retardation

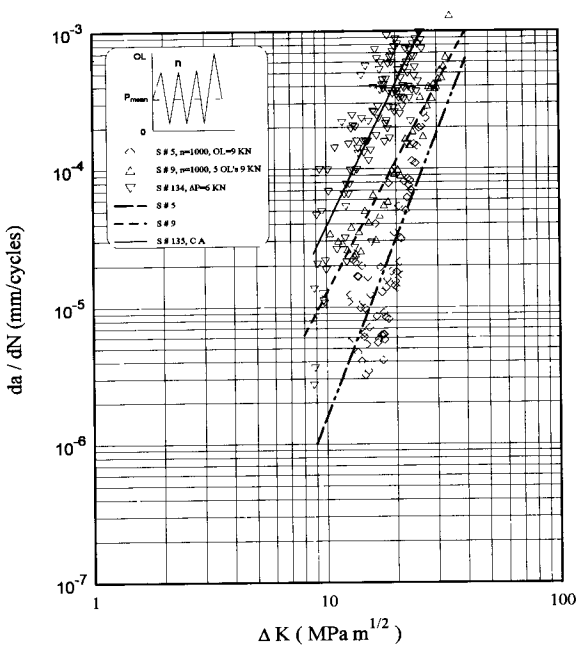

Fig. 7 FCG rate versus ΔK showing the effect of multiple overloads

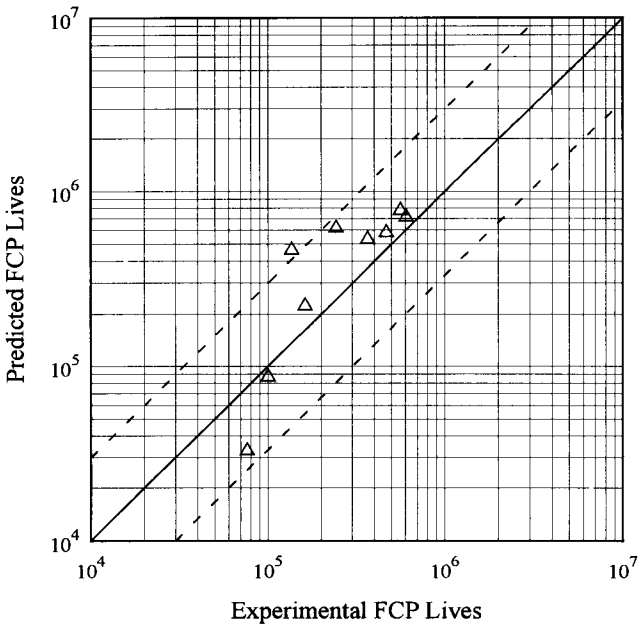

Fig. 8 Fatigue lives; experimental versus Wheeler's prediction (using modified Paris equation)

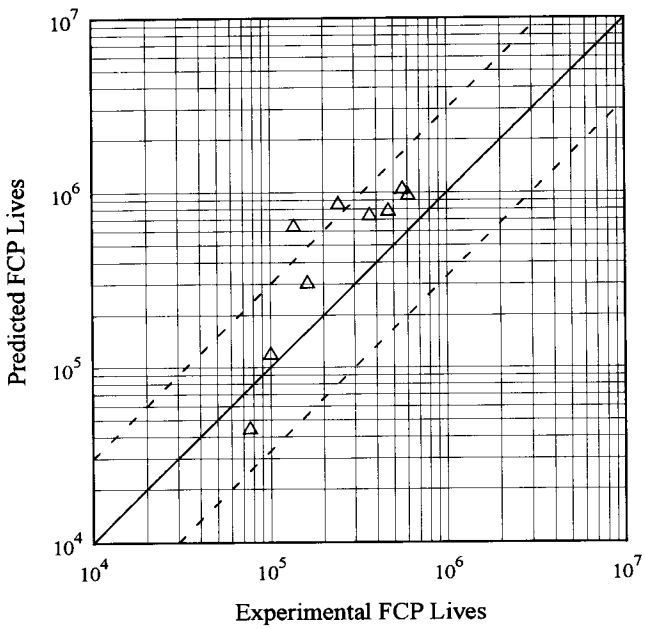

Fig. 9 Fatigue lives; experimental versus Wheeler's prediction (using Paris equation)

growth rate could be attributed to the frequency of creation of plastic zone due to increasing frequency of application of overload in the wake of the growing crack. This frequent creation of plastic zone could be considered to introduce a larger crack closure effect; thus it results in a more effective retardation of the crack growth rate. The results presented in Fig. 3 suggest that a large number of constant amplitude cycles preceding the overload causes the most pronounced retardation in the crack growth rate.

Increasing the number of overloads from one overload cycle per block to five overloads (of the same magnitude) per block causes the crack to grow at a rate faster than the growth rate where one overload cycle is applied. This suggests that the crack growth retardation effect brought by applying a single

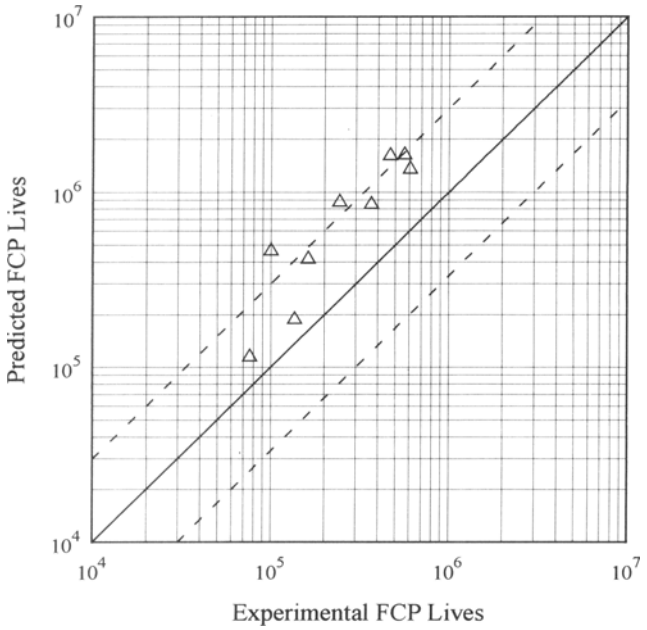

Fig. 10 Fatigue lives; experimental versus Elber's model prediction

Table 2 Material constants m and C

Sample No.	m	C, m/cycles
4	3.386	1.26×10^{-12}
5	4.32	7.52×10^{-14}
6	3.64	7.033×10^{-13}
9	3.126	8.71×10^{-12}
10	3.744	8.34×10^{-13}
11	2.58	3.306×10^{-11}
12	2.899	7.71×10^{-12}
13 CA	2.45	1.18×10^{-10}
15 CA	3.454	4.83×10^{-12}
135 CA	3.458	1.339×10^{-11}

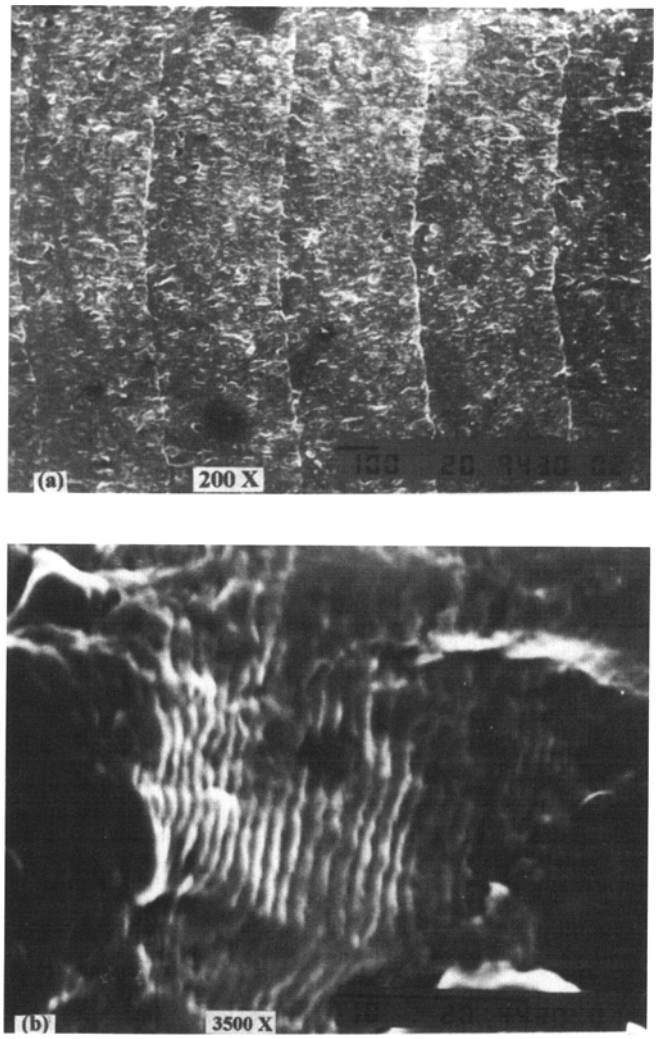

Fig. 11 Crack arrest markings (a) and fatigue striations (b) used to calculate microscopic crack growth rates

tensile overload is considerably minimized if, instead of one single tensile overload, multiple tensile overloads are applied. This observation is consistent with the expectation that crack growth acceleration is followed immediately after each overload cycle. The combined effect of the multiple overloads must be producing an appreciable amount of acceleration before the retardation takes place.

5. Fatigue Crack Propagation Lives

The predicted FCP lives calculated from the Wheeler's model using the Paris equation show good agreement with the experimental findings within a factor of three, which is a reasonably good prediction for fatigue under VAL. For n = 5000, the result is most nonconservative. These results, along with their corresponding experimental results, are shown in Fig. 8. The shaping parameter p for steel has been taken as 1.2, the geometric factor $f(g)$ as 1.12 (Ref 16, 18), a_i as per the experimental reading (around 0.001 mm), and a_f from Eq 6. The material constants m and c used in this calculation are shown in Table 2.

The predicted FCP lives calculated from Wheeler's model using the modified version of Paris equation show even better agreement with the experimental results. This improvement in the fatigue life estimation occurs due to the use of the stress ratio in the form of $(1 + R/1 - R)$ in the formulation. The modified Paris equation (Eq 8) was used for calculating the FCP lives of each sample. These results of FCP lives are presented graphically in Fig. 9.

The predicted FCP lives calculated from the Elber's model using the effective ΔK concept is more nonconservative in predicting the FCP lives when compared with the Wheeler's models (as discussed). All the data points are seen lying above the perfect correlation line (solid line). This deviation may be attributed to the inability of this model to take into account the OL ratio effect, which affects the FCP rates. Using Eq 2 and 12 and integrating gives the fatigue lives as predicted by the El-

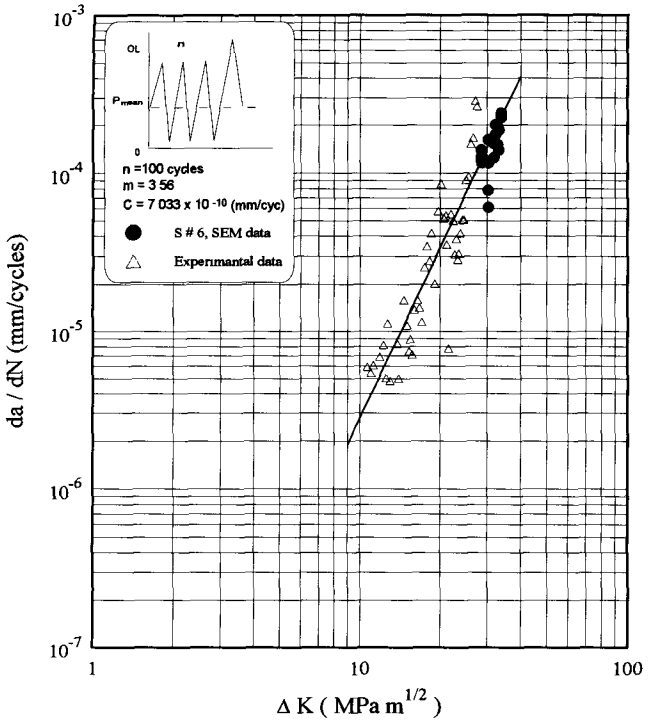

Fig. 12 Comparison of FCG rate versus ΔK (for S # 6, n = 100, 10 Hz and single overload at 9 kN) with experimental and fractographic data

ber's model. These results are also plotted against the experimental data in Fig. 10.

6. Fractographic Studies

Examination of the fractured specimen using the scanning electron microscope was conducted to correlate the experimentally observed experimental macroscopic crack growth rates with the microscopic growth rates obtained from fatigue striations. Figure 11 exhibits a fractograph taken from a specimen fatigued with a single overload cycle following the constant amplitude cycling. Figure 11(a) reveals the crack arrest marking at the application of the overload cycle. Figure 11(b) shows the typical fatigue striations found on the fracture surface of the fatigued specimen. Fatigue striation spacing observed at different positions on the fracture surface was used to calculate the microscopic crack growth rates using Eq 13. The microscopic crack growth rates were superimposed on the macroscopic crack growth rates. As shown in Fig. 12, good agreement between the macroscopic and microscopic crack growth rates has been observed.

7. Conclusions

It is clear from the results obtained here that load interaction effect under the influence of OL produces definite retardation in the fatigue crack growth rate, and consequently, the FCP life is enhanced.

Keeping the number of CAL cycles (base cycles) the same, when the magnitude of OL is increased from 9 kN (OL ratio 1.5) to 13 kN (OL ratio 2.17), the fatigue life is decreased. With the decrease in the base number of cycles (n) of CAL from 5000 to 1000, the fatigue life is decreased considerably, but further decreases in base cycle number of 100 show an increase in fatigue life compared to n = 1000 cycles and approaches that of n = 5000 cycles.

When the number of OL peaks is increased from one to five (each with the same magnitude), an acceleration in crack growth rate occurs when compared to the single OL peak. But compared to CAL, a definite retardation is observed in all cases.

Reasonably good predictions of FCP lives under VAL can be obtained using all three modified CAL models discussed. The results show that the Wheeler's model using Paris equation gives reasonable FCP life predictions under VAL conditions. Whereas the Wheeler's model using modified Paris equation improves FCP life predictions, Elber's crack closure model slightly overpredicts FCP lives for all cases.

The analytical fatigue life prediction models under VAL discussed here may be ranked as (1) modified Paris model, (2) Paris model, and (3) Elber's model.

Acknowledgment

The authors wish to gratefully acknowledge King Fahd University of Petroleum and Minerals for supporting this research.

References

1. H. Misawa, A. Fukushima, and Y. Kawakami, Effect of Very Small Number of Stress Cycles above Fatigue Limit on Fatigue Crack Propagation under Variable Amplitude Loading, *Bull. Jpn. Soc. Mech. Eng.*, Vol 28 (No. 238-3), 1985, p 578-585
2. O. Vardar, Effect of Single Over Load in Fatigue Crack Propagation, *Eng. Fract. Mech.*, Vol 30 (No. 3), 1988, p 329-335
3. Fatigue Reliability: Introduction, *ASCE J. Structural Division*, Vol 108 (No. 1), 1982, p 3-89
4. J.F. Knott and A.C. Picard, Effect of Over Load in Fatigue Crack Propagation: Aluminum Alloys, *Metall. Sci.*, Aug/Sept 1977, p 399-421
5. W.J. Mills and R.W. Hertzberg, Load Interaction Effect on Fatigue Crack Propagation in 2024-T3 Aluminum Alloy, *Eng. Fract. Mech.*, Vol 8, 1976, p 657-667
6. R.P. Wei and T.T. Shih, Delay in Fatigue Crack Growth, *Int. J. Fatigue*, Vol 10, 1974, p 77-85
7. P.J. Bernard and C.E. Richards, Methods for Comparing Fatigue Lives for Spectrum Loading, *Mater. Sci.*, 1977, p 390-398
8. K.T. Venkateswara Rao and R.O. Ritchie, Fatigue of Aluminum-Lithium Alloys, *Int. Mater. Rev.*, Vol 37 (No. 4), 1992, p 153-185
9. O. Wheeler, Spectrum Loading and Crack Growth, *J. ASME Trans.*, March 1972, p 181-186
10. J.J. Coner, J.A. Bannantine, and J. Handrock, *Fundamentals of Metal Fatigue Analysis*, Prentice Hall, 1990
11. L.P. Pook, *Developments in Fracture Mechanics*, Vol 1, Applied Science Publishers Ltd., 1983
12. R.J. Allen, A Review of Fatigue Crack Growth Characteristics by Linear Elastic Fracture Mechanics, Part III, *Fatigue Fract. Eng. Mater. Struct.*, Vol 11 (No. 2), 1988, p 45-108
13. W. Elber, "The Significance of Crack Closure," No. 486, *ASTM STP*, 1971, p 230-242
14. A. Gysler, N. Ohrloff, and G. Lutjering, Fatigue Crack Propagation Behavior under Variable Amplitude Loading, *Fatigue Crack Propagation under Variable Amplitude Loading*, J. Petit, D. David-

son, and P. Rabbe, Ed., Elsevier Science Publishers, 1988, p 24-34

15. R.E.F. Jones, Fatigue Crack Growth Retardation after Single Cycle Peak Over Load in Ti-6Al-4V, Titanium Alloy, *Eng. Mech.*, Vol 5, 1973, p 585-604
16. T. Shih and R.P. Wei, A Study of Crack Closure in Fatigue, *Eng. Fract. Mech.*, Vol 6, 1974, p 19-32
17. J.M. Barsom and S.T. Rolfe, *Fracture and Fatigue Control in Structures: Application of Fracture Mechanics*, 2nd ed., Prentice Hall, 1987
18. D.W. Hoeppner and W.E. Krupp, Prediction of Component Life by Application of Fatigue Crack Growth Knowledge, *Eng. Fract. Mech.*, Vol 6, 1974, p 47-70